Applied Geochemistry xxx (2013) xxx–xxx

Contents lists available at SciVerse ScienceDirect

Applied Geochemistry

journal homepage: www.elsevier.com/locate/apgeochem

Interaction between continental and estuarine waters in the wetlands of the northern coastal plain of Samborombón Bay, Argentina

Eleonora Carol [a,*], Josep Mas-Pla [b,c], Eduardo Kruse [a]

[a] Consejo Nacional de Investigaciones Científicas y Técnicas (CONICET), Facultad de Ciencias Naturales y Museo, Universidad Nacional de La Plata (UNLP), Calle 64 #3, 1900 La Plata, Buenos Aires, Argentina
[b] Grup de Geologia Aplicada i Ambiental (GAiA), Centre de Geologia i Cartografia Ambiental (Geocamb), Dept. Ciències Ambientals, Universitat de Girona, 17071 Girona, Spain
[c] Catalan Institute for Water Research (ICRA), 17003 Girona, Spain

ARTICLE INFO

Article history:
Available online xxxx

ABSTRACT

On the Samborombón Bay coastline, located in the Río de la Plata estuary in Buenos Aires province (Argentina), a complex hydrological system has developed at the interface between continental and estuarine water, where significant wetlands develop. The main hydrogeological units, namely the shell ridges, the tidal plain and the marsh areas, have been identified using geomorphological criteria. Water table, hydrochemical and isotopic data have been used to determine their hydrological features, as well as those of the streams and canals. Evaporation processes, in particular, have been considered when depicting chemical and isotopic changes in surface waters in streams and marsh areas. The shell ridges represent a hydrogeological unit in which rainwater is stored, constituting a lens-shaped freshwater aquifer. In this unit, just as in the tidal plain, carbonate dissolution and ion exchange are the main processes regulating water chemistry. On the other hand, in the marsh and surface waters, processes such as mixing with estuarine water and evaporation predominate. These processes control water fluxes and the salinity of the wetland areas and, consequently, their ability to preserve the existing biodiversity. This study shows the importance of knowledge of hydrochemical processes in any proposal concerning the management and preservation of this type of wetland.

1. Introduction

Wetlands are environments which combine high biomass production and rich biodiversity; consequently, they are protected worldwide by the Ramsar Convention. However, long-standing prejudices against these areas have caused the destruction of about 80% of their original extent (Custodio, 2010). Their ecological resources are now widely recognized, as well as their economic and social values (Adamus et al., 1991; Barbier et al., 1997; LePage, 2011).

Coastal wetlands, in particular, are the result of geological and hydrological processes that evolved rapidly, adapting to changing environmental conditions caused by natural or human action. Therefore, the monitoring and control of these areas are necessary requirements for their future preservation and safeguarding. Even though developing coastal areas are more likely to retain their natural characteristics, there is insufficient field information; thus, a sound description of their hydrological dynamics is necessary to ultimately address environmental planning.

Research approaches, therefore, need to provide objective descriptions in the short run to cope with the progressive human encroachment on these areas and the permanent transformation of their land uses. Hydrogeological studies, specifically those aimed at describing hydrogeochemical processes, are required to assess the present status of the area and provide insights for future sustainable development. Developers and water managers must then be committed to describing the geological, geomorphological, hydrodynamic and geochemical characteristics of coastal wetlands as it is valuable information to support management decisions.

Among the different approaches, the use of hydrochemical and isotopic data is a requirement to provide a description of wetland hydrological dynamics encompassing both continental and estuarine processes with a limited amount of data (Kruse and Mas-Pla, 2009). The purpose of this study was to investigate, on the basis of their hydrogeochemical and isotopic characteristics, the hydrological processes that govern the surface water and groundwater dynamics of wetland areas on the northern coast of the Samborombón Bay (Argentina, Fig. 1). Such hydrological knowledge is required to establish preservation criteria for water resources, their dynamics and related environmental assets in this developing coastal region.

2. Study area

The Samborombón Bay contains a wetland area that extends 180 km along the outer Río de la Plata estuary. Sea level

* Corresponding author. Tel.: +54 221 4249049; fax: +54 221 4841383.
E-mail address: eleocarol@fcnym.unlp.edu.ar (E. Carol).

0883-2927/$ - see front matter © 2013 Elsevier Ltd. All rights reserved.
http://dx.doi.org/10.1016/j.apgeochem.2013.03.006

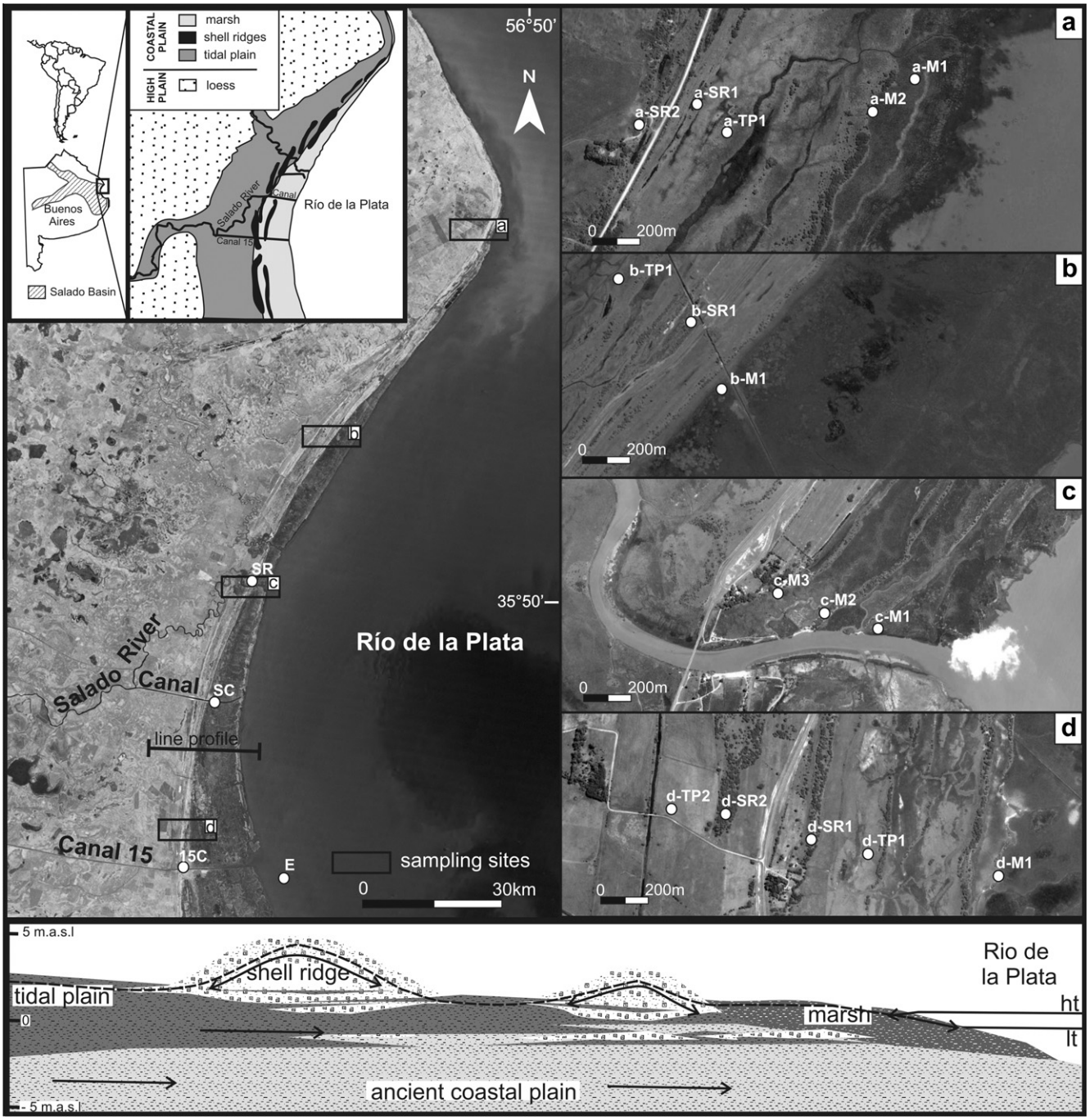

Fig. 1. Geographical location of the study area and of the sampling points in each of the transects. The lower graph shows a schematic cross-section of the main geomorphological units: shell ridges, tidal plain and coastal marshes.

oscillations during the Holocene, the sedimentary load from the Río de la Plata and coastal drift have created a vast coastal plain area that at present constitutes a large wetland zone (Violante et al., 2001; Fig. 1).

Within the coastal plain, three hydrogeomorphological units can be recognized: a tidal plain, shell ridges and a marsh (Fig. 1). The tidal plain corresponds to the coastal plain area which is currently out of the tidal cycle. The shell ridges are beach deposits occurring in high-energy environments parallel to the coastline, with a width of 50–120 m and a length that may reach up to 10 km. Within the plain environment, they constitute positive landforms with mean topographic heights of 7.5 m asl. The marsh is the portion of the coastal plain which is at present periodically flooded by the tidal flow. The marsh is 6 km wide in the central part of the bay, and 0.5 km wide in its northern sector; the altitude is <1.5 m asl. The stratigraphic basement of these deposits is made up of a Pleistocene loess formation (Parker, 1979).

The Salado River is the main watercourse in the area and flows into the Samborombón Bay (Fig. 1). This river drains the surface water from a wide depressed area that has a humid climate. The bay lies in the central part of the Salado River watershed depression and extends for more than 100 km on the west margin of the Río de la Plata. The natural drainage network is poorly developed and lacks integration (Carol et al., 2010). The mean annual rainfall is 965 mm, with March (91 mm) and June (67 mm) being the wettest and driest months, respectively. The actual evapotranspiration rate reaches

Please cite this article in press as: Carol, E., et al. Interaction between continental and estuarine waters in the wetlands of the northern coastal plain of Samborombón Bay, Argentina. Appl. Geochem. (2013), http://dx.doi.org/10.1016/j.apgeochem.2013.03.006

770 mm/a, estimated on the basis of the potential evapotranspiration by the Thornthwaite method, with the largest excess in the budget occurring in the winter months, in spite of the low precipitation (Pousa et al., 2011). High atmospheric humidity values are common all year long in the area, reaching a maximum mean value of 85% during the winter months (June–July), and a minimum value in the summer season (December–January) of approximately 75%. The almost zero slope of the area (10^{-4}) makes natural drainage towards the sea difficult. For this reason, the Salado River has been channelized in some of its reaches, namely the Salado River Canal and the Canal 15.

The Río de la Plata estuary has a microtidal regime with semidiurnal oscillations and a tidal wave range below 2 m. At high tide, alt water penetrates from the sea as a wedge underneath the freshwater of the river (Acha et al., 2008). The low height in the plain (between 1 and 5 m above sea level) makes it possible for the tidal wave to propagate towards the continent, flooding the marsh area and penetrating along the surface watercourses.

3. Methodology

3.1. Data collection

The study area includes the central and northern parts of the Samborombón Bay wetlands. As previous regional hydrological data were nonexistent, a geological and geomorphological analysis based on local maps and satellite images was carried out. From this primary information, four experimental sectors were defined. In each of them, 3-m depth boreholes were drilled along several transects perpendicular to the coastline to sample the tidal plain, shell ridges and marsh deposits (Fig. 1).

Sediment description and collection was conducted in the area to determine its mineralogical composition. Binocular laboratory microscopy and X-ray diffraction analysis using a Philips 3020 Goniometer with a PW3710 controller, Cu Kα radiation and Ni-filter, operated at 40 kV and 20 mA were used in this task.

Groundwater samples were collected from the boreholes, the Salado River and the main canals across the plain in November 2009. Sampling was conducted during low tide periods, yet specific points were also sampled at high tide. Electrical conductivity (EC), pH, major elements (HCO_3^-, CO_3^{2-}, SO_4^{2-}, Cl^-, Ca^{2+}, Mg^{2+}, Na^+, K^+) as well as Br^- and stable water isotopes ($\delta^{18}O$ and δ^2H) were determined. Sampling, preservation and analytical procedures were performed according to the Standard Methods for the Examination of Water and Wastewater (American Public Health Association, 1998). Electrical conductivity and pH were measured *in situ* after sample collection. Ion speciation and saturation indices were estimated using PHREEQC v2.13 (Parkhurst and Appelo, 1999). Ratios between chemical species were estimated using their concentrations in meq/L.

Isotopic ratios, $\delta^{18}O$ and δ^2H were measured according to the Panarello and Paricia (1984) and Coleman et al. (1982) methods, respectively, using a Finnigan MAT Delta S mass spectrometer, results are reported vs. V-SMOW (Gonfiantini, 1978). Analytical uncertainties were ±0.2‰ for $\delta^{18}O$ and ±1‰ for δ^2H.

3.2. Data interpretation

Major ion and environmental isotope data from the surface water and groundwater samples were studied together with geological and geomorphological characteristics in order to analyze the hydrogeochemical and hydrodynamic processes in the coastal plain. Estuarine water composition is also discussed as a reference for the tidal effects on surface and groundwater.

The results obtained were interpreted on the basis of ion ratio plots, saturation indices and isotopic content, contrasting the surface and groundwater samples with data from estuarine water and seawater. As there are no isotopic values for estuary samples in the study area, a value for $\delta^{18}O$ and δ^2H was estimated on the basis of the isotopic and content data for Cl^- from the middle Río de la Plata estuary (Pera-Ibarguren, 2004) and seawater (Kruse and Mas-Pla, 2009). The mean inner estuarine water isotopic signature, measured near La Plata about 120 km west of the study area, is between −3.45‰ for $\delta^{18}O$ and −18.5‰ for δ^2H (Pera-Ibarguren, 2004). Consequently, the Samborombón Bay water isotopic values may lie at some point between those data and the mean ocean value of 0‰ for $\delta^{18}O$ and δ^2H (according to the standard definition). Given a Cl^- content of 23–40 mg/L (0.6–1.1 meq/L) in the inner estuary (Pera-Ibarguren, 2004) and the mean ocean isotopic composition, an approximate isotopic content can then be estimated as a linear mixing with seawater using Cl^- data. Isotopic values of $\delta^{18}O = -2.29$‰ and $\delta^2H = -12.2$‰ can thus be assumed for Samborombón Bay water.

3.3. Evaporation modeling

In those hydrogeomorphological environments in which the evaporation processes may significantly modify water hydrogeochemistry, an evaporation model was developed to quantify such processes.

Evaporation increases the concentration of dissolved species in surface waters. Solute concentration can be estimated as a function of the fraction of evaporated water from a pond or lake. Thus, the enriched concentration C' can be estimated as

$$C' = \frac{C_0}{(1-x)} \tag{1}$$

where C_0 is the initial concentration, x is the fraction of evaporated water; i.e., $x = V/V_0$ ($0 < x < 1$), where V is the present volume and V_0 is the initial volume.

The isotopic enrichment of an evaporating surface water body based on the Craig and Gordon (1965) approach is described in detail by Gonfiantini (1986). According to Gonfiantini (1986), the isotopic composition of surface water, δ, varies as the residual or remaining fraction of the water volume, $f = V/V_0$, diminishes. The relationship between both variables is expressed as

$$\frac{d\delta}{d\ln f} = \frac{h(\delta - \delta_\alpha) - (\delta + 1)(\Delta\epsilon + \frac{\epsilon}{\alpha})}{1 - h + \Delta\epsilon} \tag{2}$$

where h is the air relative humidity; δ_α is the isotopic composition of atmospheric water vapor; α is the equilibrium fractionation factor, being the $\varepsilon = \alpha - 1$. The value of α in the liquid water–water vapor system can be expressed as a function of temperature, T in Kelvin, as defined by Kakiuchi and Matsuo (1979)

$$\ln\alpha(^{18}O/^{16}O) = 5970.2T^{-2} - 32.801T^{-1} + 0.05223. \tag{3}$$

$$\ln\alpha(^{2}H/^{1}H) = 2408T^{-2} + 65.55T^{-1} - 0.1687. \tag{4}$$

The kinetic enrichment factor, $\Delta\varepsilon$, can be adequately evaluated proportionally to the moisture deficit ($1 - h$), using

$$\Delta\epsilon\ ^{18}O‰ = 14.2(1-h) \tag{5}$$

$$\Delta\epsilon\ ^{2}H‰ = 12.5(1-h) \tag{6}$$

After an appropriate integration, and defining δ_0 as the initial isotopic composition of water at $f = 1$, the Gonfiantini (1986) expression for $\delta(f)$ turns to the following equation:

$$\delta = \left(\delta_0 - \frac{A}{B}\right)f^B + \frac{A}{B} \tag{7}$$

Please cite this article in press as: Carol, E., et al. Interaction between continental and estuarine waters in the wetlands of the northern coastal plain of Samborombón Bay, Argentina. Appl. Geochem. (2013), http://dx.doi.org/10.1016/j.apgeochem.2013.03.006

with the terms A and B given by

$$A = \frac{h\delta_\alpha + \Delta\epsilon + \epsilon/\alpha}{1 - h + \Delta\epsilon} \quad (8)$$

$$B = \frac{h - \Delta\epsilon - \epsilon/\alpha}{1 - h + \Delta\epsilon} \quad (9)$$

Taking the isotopic balance of a well-mixed lake undergoing evaporation, Gonfiantini (1986) presents the equation of lake-water isotopic composition as a function of the ratio between the net evaporation rate (E) and the lake inflow (I), $x = E/I$ and $0 \leqslant x \leqslant 1$, for those cases where the lake volume does not change significantly with time ($dV/dt = 0$) (Eq. (10))

$$\delta_L = \left(\frac{\delta_1 + Ax}{1 + Bx}\right) \quad (10)$$

where δ_1 is the mean isotopic composition of the lake inflow. The value δ_L reflects the isotopic equilibrium between inflow and evaporation rates under kinetic fractionation. If no evaporation occurs ($x = 0$), δ_L becomes equal to δ_1. For those cases where the lake volume varies along the evaporation processes, if the inflow becomes negligible, the evolving lake-water isotopic composition may be estimated using Eq. (7) and simply considered as an evaporating mass of water.

4. Results

The samples analyzed were of shallow groundwater and surface water from the Salado River and its associated canals, as well as samples of estuarine water. Regarding shallow groundwater, each unit in the coastal plain (i.e., tidal plain, shell ridge and marsh) was considered as a hydrogeological unit with specific hydrodynamic and hydrochemical characteristics.

4.1. Surface water

As a reference, two samples of estuarine water from the central sector of the Samborombón Bay show a clear Na^+–Cl^- facies (Fig. 2), with a salinity below 15,000 mg/L (Table 1). These samples have Na^+/Cl^+, Mg^{2+}/Cl^-, and Ca^{2+}/SO_4^{2-} ratios similar to those of seawater (Fig. 3), although they show an average dilution of 35% with regard to mean ocean Cl^- content. The Ca^{2+}/HCO_3^- ratio in estuarine water is higher than the one in seawater, a characteristic which reflects the influence of the contribution of the Río de la Plata.

In the littoral area, oscillations are recorded in the water level of the Salado River and the canals depending on the tidal cycle in the estuary. Measurements of flow direction in the sampling points (Fig. 1) indicate water inflow from the estuary towards the continent at high tide. This interaction area between continental and estuary flows reaches a width of approximately 5 km, which increases considerably during storm events or extraordinary high tides.

The hydrochemistry of the Salado River and canals close to the coastline also shows a clear Na^+–Cl^- facies (Fig. 2), with salinities ranging from 3710 to 6950 mg/L. Sodium concentration grows linearly with Cl^-, and their relationship is 1.1–1.3, showing a slight Na excess compared to estuarine water (Fig. 3). The close similarity of the Na^+/Cl^- ratio with that of estuarine water indicates that most of the Na and Cl^- can be attributed to tidal influence. These samples also show a surplus of HCO_3^- and SO_4^{2-} compared to Ca,

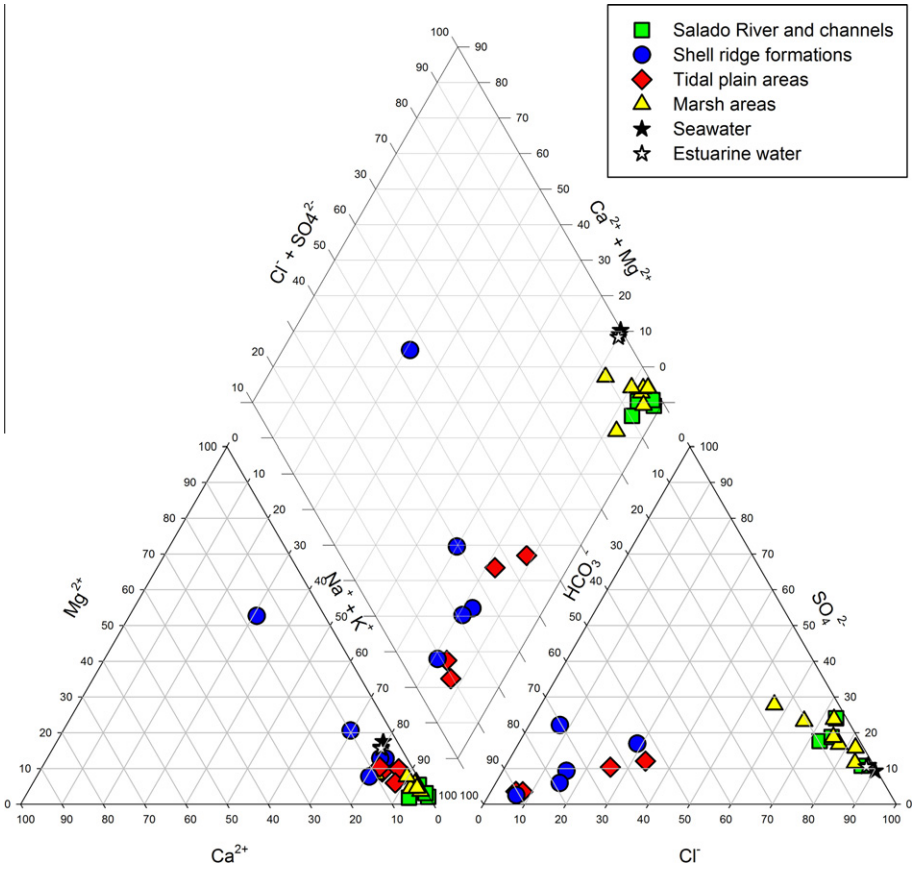

Fig. 2. Piper diagram of the surface water and groundwater samples from the Samborombón Bay coastal wetlands. Seawater in all plots is just plotted for comparison, as it does not contribute to the hydrochemistry of the study area.

Please cite this article in press as: Carol, E., et al. Interaction between continental and estuarine waters in the wetlands of the northern coastal plain of Samborombón Bay, Argentina. Appl. Geochem. (2013), http://dx.doi.org/10.1016/j.apgeochem.2013.03.006

with Ca^{+}/HCO_3^- ratios between 0.09 and 0.81, and Ca^{2+}/SO_4^{2-} ratios between 0.02 and 0.27. Such a wide range of ratios suggests the influence of groundwater input on stream discharge. The content of Cl^- and Br^- show little variation, with the Br^-/Cl^- ratio ranging from 8.22×10^{-5} to 3.03×10^{-4} (Fig. 4).

Different mixing proportions between continental and estuarine water are shown by, for instance, the range of Cl^- concentrations found in the Salado River and its canals. These samples show undersaturation with respect to calcite, gypsum and halite (Fig. 5). The wide range of SI values for calcite and gypsum reflects the variability of Ca^{2+} and HCO_3^- concentration during mixing between estuarine and continental waters, as well as calcite equilibrium under atmospheric (open-system) conditions. A progressive increase in Cl^- causes an increase of the saturation index of halite.

Isotopic data for the stream water of the Salado River and drainage canals vary between −0.60‰ and −1.90‰ for $\delta^{18}O$, and −5.0‰ and −12.0‰ for δ^2H (Fig. 6), which are heavier than those of estuarine water. Stream values deviate noticeably from the local meteoric water line (LMWL: $\delta^2H = 8\ \delta^{18}O + 14$; Dapeña and Panarello, 2004; Fig. 6) and this shift is attributed to evaporation processes as isotopic data are even more enriched than estuarine water. Sea water isotopic composition is added in Fig. 6 for reference; however, there is no 'pure' sea water in the Samborombón Bay, but estuarine water; so mixing with sea water is not a feasible option to explain stream water isotopic data. In later discussion, Fig. 7 shows a trend in the Cl^- vs. $\delta^{18}O$ plot that indicates the occurrence of evaporation.

In this paper, the evaporation process is quantified using the Gonfiantini (1986) equations to estimate the rate of evaporation, as well as additional aspects of this hydrological system. Eq. (7), which corresponds to an evaporating water body, is used to reproduce the evaporation path of a stream sample, assuming that tidal processes result in a well-mixed mass of water. The initial isotopic composition of the Salado River is estimated on the basis of the mixing percentage, calculated according to the Cl^- balance (35% estuarine water and 65% continental discharge). If the content estimated for the estuary in the study area is $\delta^{18}O = -2.29‰$, and $\delta^2H = -12.2‰$ and the isotopic content of the continental discharge is regarded as being determined by the mean value of the groundwater samples with no tidal influence discharging into the river and canals ($\delta^{18}O = -5.30‰$, and $\delta^2H = -30.0‰$), the initial isotopic composition of the Salado River (δ_0) for a mixing proportion 0.35/0.65 is $\delta^{18}O = -4.25‰$, and $\delta^2H = -23.8‰$.

This initial isotopic composition of the water, with a relative humidity of 0.85, a mean temperature of 20 °C, and an isotopic composition of the atmospheric vapor of $\delta^{18}O = -12‰$, and $\delta^2H = -86‰$ has been considered to reproduce the observed values. The evaporation trend, at a relative humidity of 0.85, indicates that the isotopically heavier river samples are consistent with the predicted evolution, and that evaporation represents 15–20% of the total volume (Fig. 6).

This evaporation trend affecting chemical and isotopic data also reproduces the measured river data in the Cl^- vs. $\delta^{18}O$ plot (Fig. 7). Two trend lines, corresponding to the mean relative humidity of 0.85 and that of 0.93, starting at the mentioned δ_0 value, are shown in the plot. Given the arbitrary values of atmospheric vapor, the line at $h = 0.850$ has a larger asymptotic value of $\delta^{18}O$, whereas that at $h = 0.93$ results in a better simulation of both chemical and isotopic data.

4.2. Groundwater in the tidal plain

Tidal plains are nowadays free of estuarine influence. Borehole logs show sand and silt layers, and clay levels with shell

Table 1
Hydrochemical (mg/L) and isotopic data (‰) for the Samborombón Bay coastal area.

Sample		TDS	pH	HCO_3^-	SO_4^{2-}	Cl^-	Br^-	NO_3^-	Ca^{2+}	Mg^{2+}	Na^+	K^+	Error	$\delta^{18}O$	δD
Estuarine water															
E1		12,780	8.10	151	1040	6182	nd	75	178	367	3410	65	−2.74	nd	nd
E2		14,745	7.80	272	1184	7273	nd	120	222	432	4100	89	−1.93	nd	nd
Surface water															
SR		4770	7.96	478.3	1152	3391	1.9	2.6	128	28	2685	74.1	−0.07	−0.6	−6.0
SR−ht		6950	7.74	167.1	1281	2890	0.67	2.7	8.9	41.3	2416	74.1	−0.07	−1.9	−12.0
SC		6410	7.99	388.6	1118	6638.5	1.23	2.5	9.8	54.6	4821	78	−0.07	−0.6	−5.0
15C		3710	7.85	568	820	2485	1.7	12.9	16	63.2	2039	66.5	−0.17	−0.8	−6.0
Groundwater															
Marsh	a-M1	9310	7.07	399	2648	10,188	0.65	0.5	120	194	7416.8	163.8	−0.05	−3.5	−21.0
	a-M2	8220	7.51	747	1920	5693	1.4	0.7	110	199	4316.5	117	−0.05	nd	nd
	b-M1	1730	6.91	233	402	844	1.1	8.9	70	36.5	647.3	50.7	−0.28	−4.6	−28.0
	b-M1-ht	1670	nd	nd	nd	1089	1	nd	nd	nd	nd	nd	nd	−4.6	−28.0
	c-M1	8480	7.17	872	2160	7380	1.4	0.5	68	119.5	5759.5	136.5	−0.04	nd	nd
	c-M2	9310	6.9	514	3130	7099	1.2	0.5	90	189	5738.4	156	−0.04	−3.3	−23.0
	c-M3	1360	7.38	396.6	560	841	1.7	5.7	28	22.8	868.8	31.2	−0.16	nd	nd
	d-M1	23,500	7.20	1345	2928	15,815	1.9	3.5	122	389	11,100	281	−0.10	nd	nd
Tidal Plain	a-TP1	964	7.88	274.8	35	64	1.5	11.5	11	8.9	125.1	12.2	−1.45	−5.0	−27.0
	b-TP1	526	7.33	397	69	140.6	0.86	11.6	15	8.6	232.6	12.5	−0.89	nd	nd
	b-TP1-ht	522	nd	nd	nd	73.5	0.05	nd	nd	nd	nd	nd	nd	−6.2	−38.0
	d-TP1	539	7.20	795	24.8	31.6	0.42	9.7	10	17.4	278	15.6	−0.61	−4.3	−25.0
	d-TP1-ht	510	nd	nd	nd	35.1	0.21	nd	nd	nd	nd	nd	nd	−4.4	−23.0
	d-TP2	380	7.18	478	14.9	24.6	0.35	3.5	14	9.7	160	15.6	−0.24	nd	nd
	d-TP2-ht	309	nd	nd	nd	14	0.32	nd	nd	nd	nd	nd	nd	−5.1	−29.0
Shell ridge	a-SR1	285	7.41	181	44.6	56	0.42	18.4	18	35	34.1	7.8	−2.81	−5.0	−26.0
	a-SR2	222	7.37	244.4	14.5	28.2	0.67	9.9	12	4.8	85.6	15.6	−1.49	−5.0	−29.0
	b-SR1	343	7.76	395	98	24.6	0.8	7.8	18	23	133	23.4	−0.91	−5.5	−32.0
	b-SR1-ht	403	nd	nd	nd	77.3	0.58	nd	nd	nd	nd	nd	nd	nd	nd
	d-SR1	209	7.38	263	25.7	31.6	0.2	0.9	6	8.9	103.5	7.8	−0.18	−5.3	−33.0
	d-SR2	278	7.60	406	8.9	17.6	0.05	15.5	9.5	11.4	130	9.2	−1.91	−5.3	−34.0

SR: Salado River; M: marsh areas; TP: Tidal Plain areas; SR: shell ridge areas; ht: high tide; nd: not determined. Errors based on % ionic balance. See sample location (a, b, c, d) in Fig. 1.

Please cite this article in press as: Carol, E., et al. Interaction between continental and estuarine waters in the wetlands of the northern coastal plain of Samborombón Bay, Argentina. Appl. Geochem. (2013), http://dx.doi.org/10.1016/j.apgeochem.2013.03.006

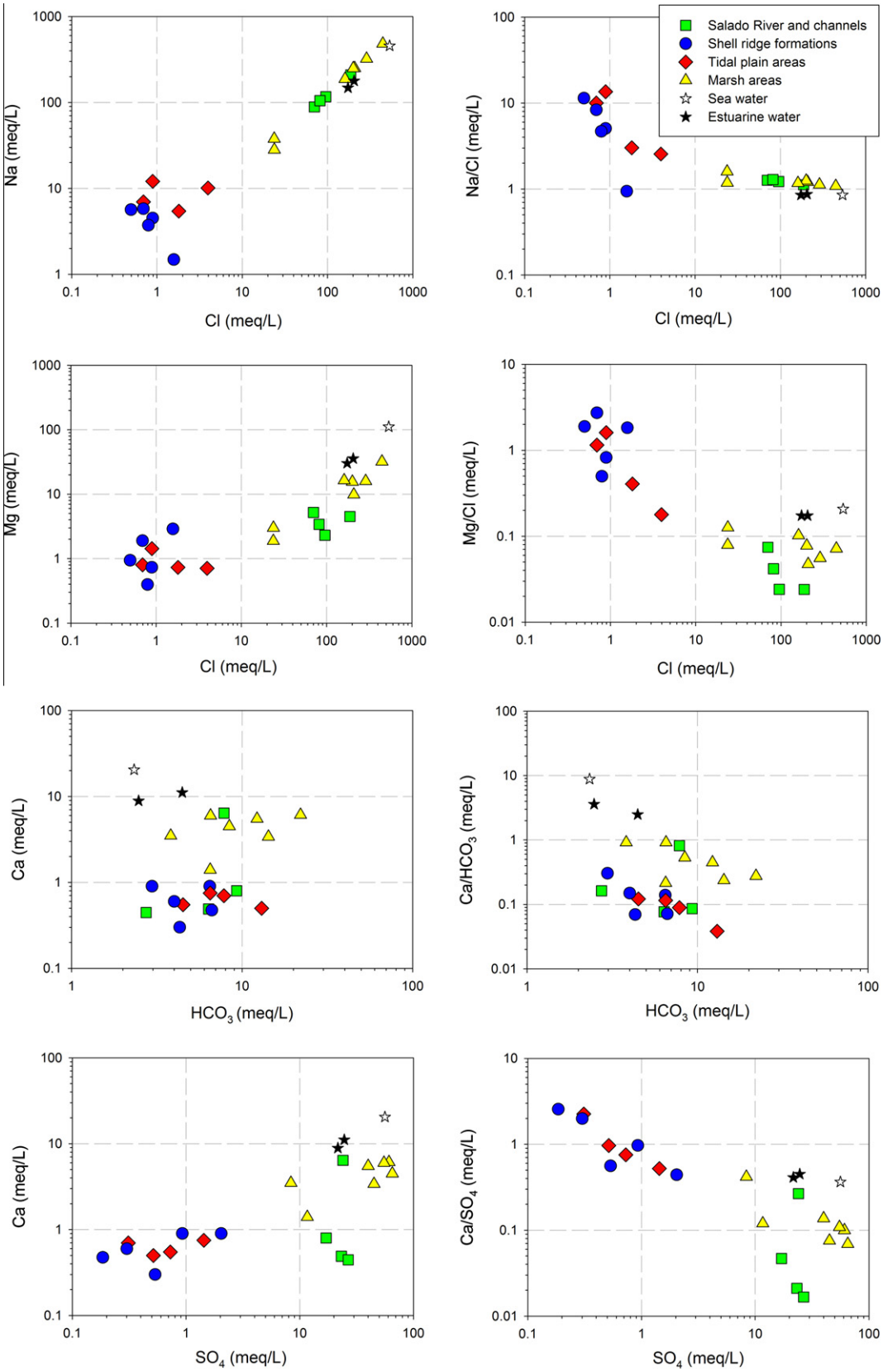

Fig. 3. Bivariate hydrochemical relations between selected parameters, expressed in meq/L, and their ratios.

Please cite this article in press as: Carol, E., et al. Interaction between continental and estuarine waters in the wetlands of the northern coastal plain of Samborombón Bay, Argentina. Appl. Geochem. (2013), http://dx.doi.org/10.1016/j.apgeochem.2013.03.006

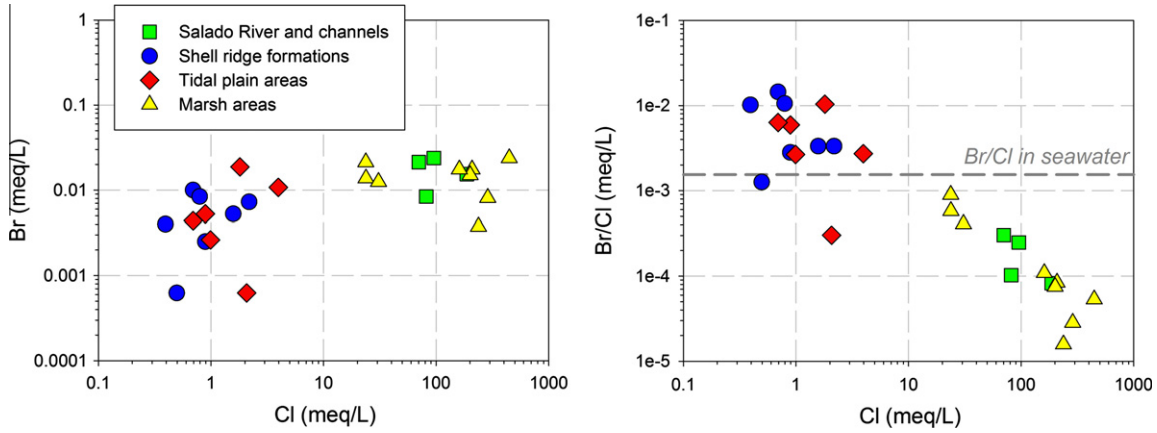

Fig. 4. Chloride–Br^- plot of the surface water and groundwater samples from the Samborombón Bay coastal wetlands. The Br^-/Cl^- ratio in seawater is plotted for reference (Edmunds, 1996).

intercalations. Coarse sand is formed by quartz and sodic plagioclase clasts, as well as fragments of carbonate shells (Table 2). The water table is between 1.0 and 1.5 m asl in the westernmost areas and it decreases to 0.7 m asl towards the coast, showing groundwater flow towards the bay, river and canals (Fig. 1).

Groundwater in the tidal plain areas shows a Na^+—HCO_3^- facies, also with low salinity (380–964 mg/L; Fig. 2; Table 1). Sodium is the most abundant cation (up to 278 mg/L), contrasting with the low concentration of Ca and Mg, which have maximum values of 15 and 17 mg/L, respectively. As in the shell ridge hydrochemistry, there are high HCO_3 concentrations with respect to Cl^- and SO_4^{2-}, in equilibrium with calcite.

The Na^+/Cl^- ratio decreases from 13.5 to 2.6 as the Cl^- content increases from 0.90 to 3.97 meq/L (Fig. 3). An increase in HCO_3^- can be observed, associated with Ca^{2+}/HCO_3^- values between 0.04 and 0.12, whereas the SO_4^{2-} content shows little variation and the Ca^{2+}/SO_4^{2-} ratio increases from 0.56 to 2.25 (Fig. 3). The low Cl^- content is associated with Mg^{2+}/Cl^- ratios of between 0.17 and 1.6 and with Br^-/Cl^- ratios between 0.01 and 3.02×10^{-4} (Figs. 3 and 4).

Saturation indices for calcite, gypsum and halite for the tidal plain samples are similar to those from the shell ridge areas, yet the concentrations of the main anions are slightly larger in the tidal plain (Fig. 5).

The δ^2H varies between −38‰ and −23‰, while $\delta^{18}O$ between −4.3‰ and −6.2‰, with the samples being located along the local meteoric water line with a slight displacement towards the evaporation line (Fig. 6). The ^2H excess values range between −11.6‰ and −13.0‰, showing that isotopic enrichment is associated with slightly variable Cl^- values (Fig. 7).

Positive values of Na^+—Cl^- and negative values of $(Ca^{2+} + Mg^{2+}) - (SO_4^{2-} + CO_3^{2-} + HCO_3^-)$ are linearly related, lying along the straight line 1:1 with a correlation coefficient of −1.00 (Fig. 8), indicating exchange processes of Na^+ for Ca^{2+}.

4.3. Groundwater in the marsh

Marsh areas are composed of sand layers embedded in silt–clay formations where the organic soil is inhabited by thousands of burrowing crabs; an example of marsh biological activity. The main minerals (Table 2) in the silt–clay sediments are quartz, basic plagioclase, $CaCO_3$ of organic origin (shells) and mineral deposits. These sediments are linked to anoxic environments located below the water table as indicated by green clay horizons and the occurrence of pyrite.

The water table is at the ground surface or very close to it, reaching a maximum depth of 0.6 m below ground surface and having periodic tidal oscillations. Groundwater flow is usually towards the bay, yet the marsh areas are commonly flooded during high tides, which control the overall groundwater infiltration and regional flow paths. Indeed, halite precipitation has been observed during dry periods, indicating the occurrence of complete evaporation as well as an available solid phase for further dissolution (Fig. 9a).

The groundwater hydrochemical facies is Na^+–Cl^- with very high salinity and a maximum value of 23,500 mg/L. Median pH value is 7.17; the Cl^- content varies between 841 and 15,815 mg/L, whereas the Na^+ content ranges from 647 to 11,100 mg/L, with prominently high SO_4^{2-} contents, reaching 3130 mg/L (Table 1).

The Cl^- content increases proportionally with the Na^+, with a Na^+/Cl^- ratio close to 1 and a trend towards seawater. The Ca^{2+}/HCO_3^- ratio decreases as the concentration of HCO_3^- increases (from 3.81 to 22.04 meq/L). The increase in SO_4^{2-} (from 8.37 to 60.96 meq/L) is associated with slightly variable Ca^{2+}/SO_4^{2-} values, showing SO_4^{2-} excess higher than that in seawater in most samples. A similar behavior can be observed in the Mg^{2+}/Cl^- ratio, which maintains values between 0.04 and 0.10 when the Cl^- content increases (Fig. 3). In turn, all the samples show a Br^-/Cl^- ratio below the one in seawater, varying between 8.96×10^{-4} and 1.58×10^{-5} (Fig. 4). The deficiency in Ca^{2+} and Mg^{2+} with respect to SO_4^{2-} and HCO_3^- is higher than the Na^+ excess with respect to Cl^- (Fig. 8).

The SI for calcite tends to increase (between −1.56 and 0.02) as the HCO_3^- concentrations increase. The SI for gypsum (between −1.61 and −0.94) with respect to SO_4^{2-} shows a trend towards seawater but with lower SI values. Even though the SO_4^{2-} content is high, the low Ca^{2+}/SO_4^{2-} ratio (close to 0.1) in most of the samples causes the SI to be negative. With regard to halite, the SI (between −4.90 and −2.56) with respect to Cl^- has a trend towards seawater, with SI and Cl^- values in several samples being similar to the ones in estuary water (Fig. 5).

The isotopic values vary between −2.30 and −4.60 for $\delta^{18}O$‰ and between −20.0 and −28.0 for δ^2H‰, with the samples being located along the evaporation line, between the intersection with the meteoric water line and seawater (Fig. 6). The $\delta^{18}O$‰ ratio with respect to Cl^- shows isotopic enrichment together with an increase in Cl^-, with a trend towards seawater (Fig. 7).

The marsh samples show a higher Cl^- content than that of estuarine water (Fig. 3), and their isotopic composition may indicate some incipient evaporation (Fig. 6); but a joint chemical-isotopic evaporation line could not be successfully reproduced in Fig. 7.

4.4. Groundwater in the shell ridges

Shell ridges are hydrogeomorphological units where the water table tends to follow the topography, with values in the studied

Please cite this article in press as: Carol, E., et al. Interaction between continental and estuarine waters in the wetlands of the northern coastal plain of Samborombón Bay, Argentina. Appl. Geochem. (2013), http://dx.doi.org/10.1016/j.apgeochem.2013.03.006

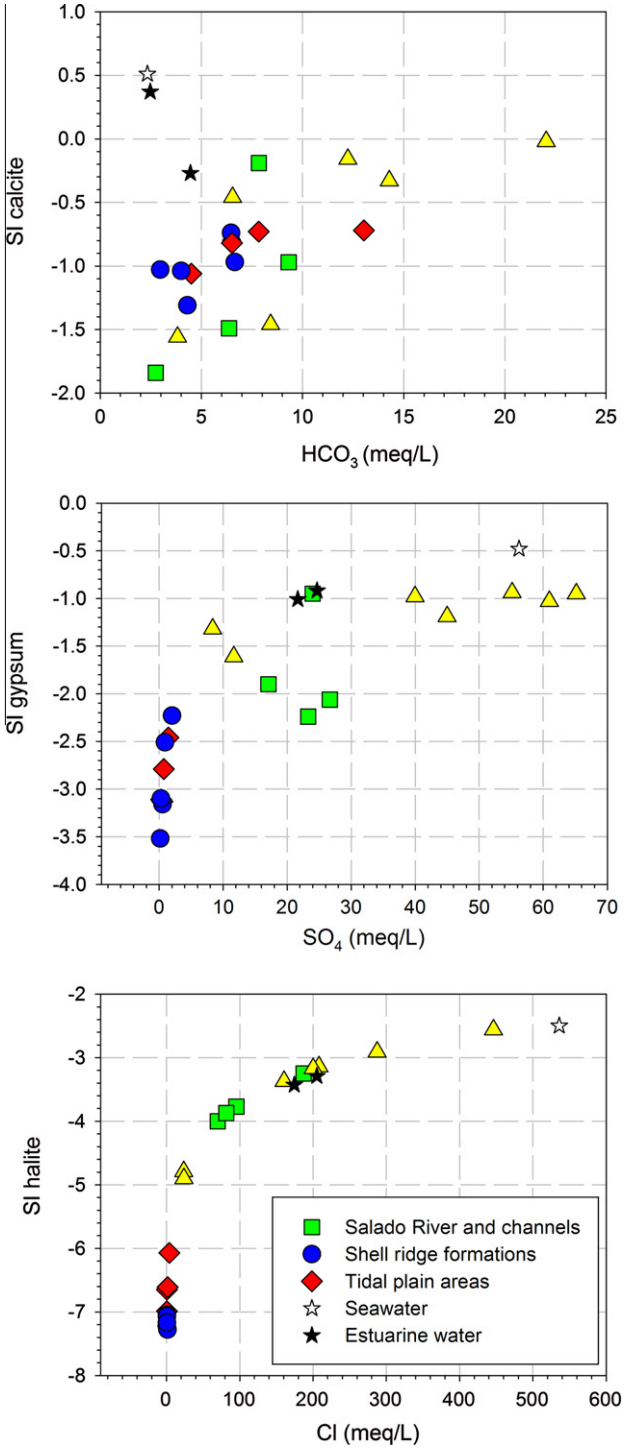

Fig. 5. Saturation indices of calcite, gypsum and halite with respect to their main anions: HCO_3^-, SO_4^{2-} and Cl^-, respectively.

ridges between 3 and 5 m asl; groundwater flows from the crest of the ridges towards the edges (Fig. 1). Shell ridges are constituted by shell fragments and post-sedimentary calcite precipitation, as well as sand layers with quartz and feldspar (basic plagioclase) minerals (Table 2). Some 0.5-m-thick clay layers can also be found within the shell deposits (Fig. 9b). The high permeability of the sediments favors rainfall infiltration processes, resulting in areas of preferential recharge. The positive morphology of the ridges and their capacity to store rainwater cause freshwater lenses to occur in this hydrogeological unit above the more saline units (i.e., the tidal plain and marsh).

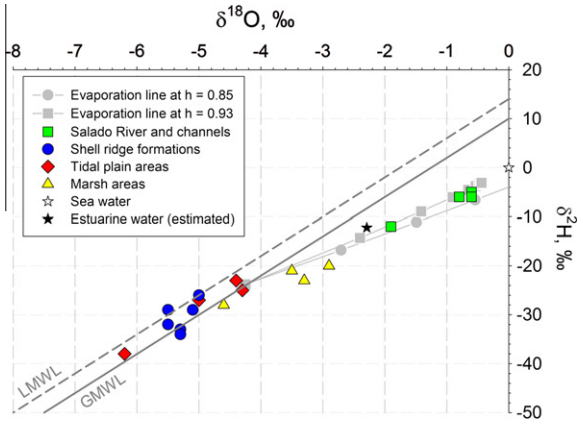

Fig. 6. Isotopic plot of the surface water and groundwater samples from the Samborombón Bay coastal wetlands. Evaporation lines for distinct values of air relative humidity, in a hypothetical mixed sample between estuarine and continental waters, showing the evolution of the Salado River and canal samples (see text).

Groundwater is generally of low salinity (<350 mg/L), neutral pH (about 7.5) and Na–HCO_3 facies (Fig. 2; Table 1), with Na^+ and HCO_3^- concentrations between 34 and 133 mg/L, and 181 and 406 mg/L, respectively. Chloride and SO_4^{2-} contents are low, and Ca (6–18 mg/L) is below the estimated ranges for carbonate formation where equilibrium with calcite was expected. Bicarbonate increases independently of Ca, with low Ca^{2+}/HCO_3^- ratios. The predominance of Na^+ as a cation and the low Cl^- content gives a high Na^+/Cl^- ratio, usually above 1, reaching values as high as 11.4 (Fig. 3). In turn, the Br^-/Cl^- ratio is higher than the one in seawater, except for one sample (Fig. 4). The low Cl^- content indicates little interaction with estuarine water, consistent with the flow distribution in the shell ridges. Moreover, Fig. 8 shows an excess of Na^+ compared to Cl^- (caused by positive values of Na^+–Cl^- between 0.01 and 5.16), as well as a deficiency of Ca^{2+} and Mg^{2+} compared to HCO_3^- and SO_4^{2-} (with negative values between 0.12 and −5.72 for $(Ca^{2+} + Mg^{2+}) - (SO_4^{2-} + CO_3^{2-} + HCO_3^-)$, displaying a linear correlation (r^2) of 0.99 (Fig. 8). This suggests that cation exchange may occur within these deposits. This process also appears to affect other groundwater samples, such as those from the tidal plain and marsh areas.

Saturation indices are below zero, indicating undersaturation for calcite, gypsum and halite, especially for these last two minerals, as a result of the deposit mineralogy (Fig. 5). Cation exchange ($H_2O + CaCO_3 + 2Na\text{-}X \leftrightarrow X_2{-}Ca + 2Na^+ + HCO_3^- + OH^-$) contributes then to the decrease of SI for calcite and gypsum, and it may also explain a pH as high as 7.75 for the sample with a higher calcite SI, according to Appelo (1994).

The environmental isotopes vary between −5.00‰ and −5.50‰ for $\delta^{18}O$, and between −26.0‰ and −34.0‰ for δ^2H, with most of the samples being located along the local meteoric water line ($\delta^2H‰ = 8\ \delta^{18}O‰ + 14$) (Dapeña and Panarello, 2004, Fig. 6). Isotopic differences in the shell ridge samples are attributed to rainfall isotopic variability, which is consistent with a fast piston-like flow groundwater recharge as expected in these highly permeable formations. The relationship between $\delta^{18}O$ and Cl^- shows a trend towards isotopic enrichment, with no increase in Cl^- (Fig. 7) and a ^2H excess ranging between 8.4‰ and 14.0‰.

5. Discussion

The hydrological complexity of the wetland with regards to the hydrogeochemical and hydrodynamic processes affecting it is shown in Fig. 10. The surface estuarine water (SWE) is characterized

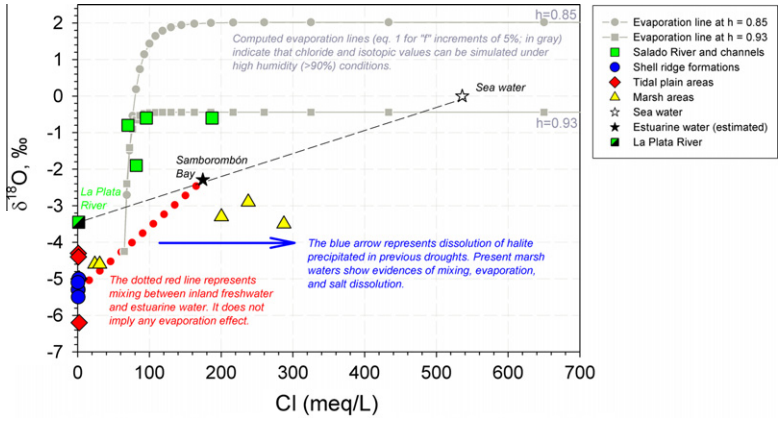

Fig. 7. Chloride vs. $\delta^{18}O$ plot. Lines show isotopic and chemical modeling of the evaporation processes, as well as mixing and salt precipitation identified in the Samborombón Bay wetlands. Data for the Río de la Plata samples from Pera-Ibarguren (2004), and estuarine water data are estimated values (see text).

Table 2
Mineral phases present in the sediments (qualitative determination by X-ray).

	Quartz	Sodic plagioclase	Carbonate shells	Pyrite
Tidal plain	x	x	x	
Marsh	x	x	x	x
Shell ridges	x	x	x	

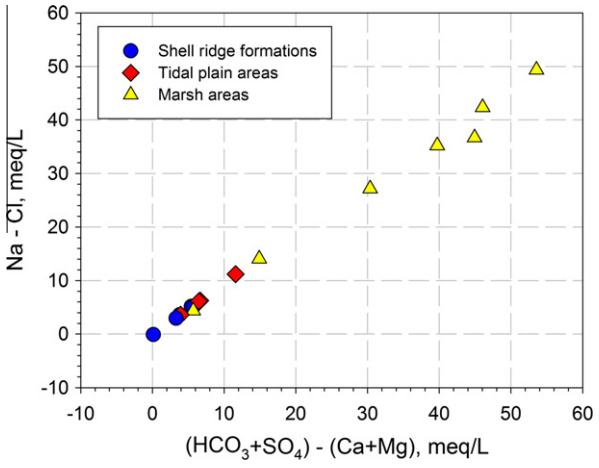

Fig. 8. Relationship between main cation and anion concentration differences illustrating cationic exchange in groundwater samples.

by the predominance of continental discharge and the influence of seawater at high tide, whereas in the Salado River and its canals (SWRC), groundwater discharge, estuarine water mixting and evaporation are the dominant processes. As for groundwater, even though similar processes prevail in the shell ridges (GWSR) and the tidal plain (GWTP), i.e., rainfall recharge, dissolution of $CO_{2(g)}$, dissolution of carbonate, and Na^+/Ca^{2+} exchange, the differences in lithological composition in both units result in differential hydrochemical characteristics. Processes of estuarine water mixture, evaporation, dissolution of halite and dissolution of pyrite predominate in the marsh (GWM).

Surface water from the Salado River and canals indicates the influence of tidal flows that flood the wetland area and then return through the drainage network to the bay. Hydrochemical ratios and isotopic data provide evidence of the occurrence of such mixing between continental water and estuarine tidal flows (Fig. 10). In particular, Cl^- data for surface water shows that it may originate from mixing of continental discharge and estuarine tidal inputs, with a 65/35 ratio contribution, respectively. Isotopic modeling shows that 15–20% of the total stream water evaporates.

Marsh areas are related to present tidal processes and they become flooded during high tides. The intense burrowing activity of different invertebrate species, such as crabs, enhances estuarine water infiltration to the subsoil (Carol et al., 2011). Element ratios of marsh groundwater samples are close to those of estuarine water, and, as well as their high salinity, corroborate the influence of the estuarine input. Chloride, SO_4^{2-} and Na^+ contents are high as a result of seawater influence during high tides and, more interestingly, their contents may be even higher than those of the estuarine samples. Even halite solubility indices are above those for the estuarine water. Thus, the Na^+/Cl^- ratio for marsh samples is slightly above 1.0, as opposed to the estuarine waters which, consistent with seawater, show a Na^+/Cl^- ratio lower than 1.0. Moreover, Cl^-, SO_4^{2-} and Mg^{2+} concentrations in most of the marsh samples are larger than those in estuarine water.

Marsh area samples show the highest saturation indices for calcite, gypsum and halite, which can be explained by hydrological behavior that alternatively encompasses flood and drought periods. In addition, isotopic values are lighter than the mean estuarine value previously extrapolated, thus supporting the supposition that marsh water originates from a mixing between continental and estuarine waters with a major contribution from the former end member.

The Br^-/Cl^- relationship is a distinguishing feature of the hydrogeological units that have no relationship with the dynamics of the estuary (i.e., the shell ridge and tidal plain areas). Unfortunately, no Br^- data are available for the estuarine samples, although sample associations can be clearly observed in this bivariate plot. In general, samples from the Salado River and canals, as well as those from the marsh areas, show severe Br^- depletion. The preferential uptake of Br^- over Cl^- in marsh areas (Barros et al., 2008) may provide an explanation for the decrease in the Br^-/Cl^- ratio.

All these differences contribute to the distinct hydrological processes in the marsh area (Fig. 10), namely, the mixing between continental and estuarine water and the dissolution of halite precipitated on the marsh floor, as well as other evaporate minerals formed during dry periods. Field evidence indicates that marsh areas undergo severe evaporation that contributes to the total desiccation of the water. As a result, halite and other evaporate minerals form in the salt-rich soils. The initial chemical and isotopic composition in the marsh can be defined as a linear mixing between the estimated estuarine water parameters and those from

Please cite this article in press as: Carol, E., et al. Interaction between continental and estuarine waters in the wetlands of the northern coastal plain of Samborombón Bay, Argentina. Appl. Geochem. (2013), http://dx.doi.org/10.1016/j.apgeochem.2013.03.006

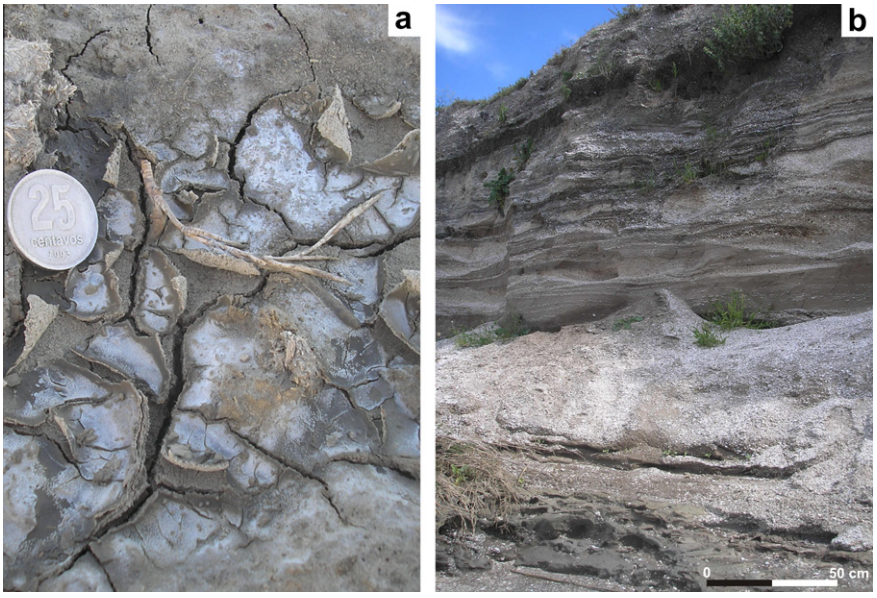

Fig. 9. (a) Halite precipitation and mud cracks after an intense evaporation period in a marsh pond; (b) example of a shell-ridge outcrop with unmixed shell and silt layers.

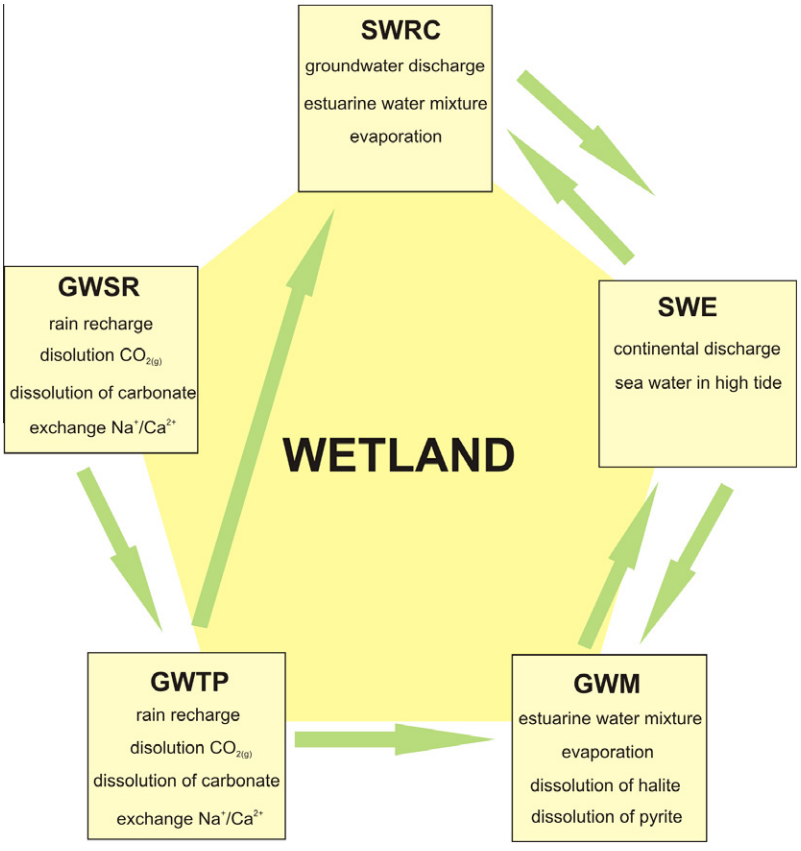

Fig. 10. Diagram indicating the main hydrogeochemical processes (boxes) and the hydrodynamic interactions (green arrows) in each hydrological environment of the wetland; SWRC, Salado River and canal surface water; SWE, estuarine water; GWTD, tidal plain groundwater; GWM, marsh groundwater; GWSR, shell ridge groundwater. (For interpretation of the references to colour in this figure legend, the reader is referred to the web version of this article.)

continental waters, represented by the shell ridge water samples. According to its geomorphological characteristics, a distinct contribution from each end member could be expected in each water body, as indicated by the two groups of marsh samples differentiated by all of the ionic and isotopic ratio parameters.

Such mixed waters experience evaporation and, therefore, chemical and isotopic changes. Nevertheless, none of the evaporation models (Eqs. (7) and (10)) could simulate a trend that would reproduce samples with a Cl^- concentrations > 200 meq/L and $\delta^{18}O$ around −3.0‰. Both evaporation trends, starting at any

Please cite this article in press as: Carol, E., et al. Interaction between continental and estuarine waters in the wetlands of the northern coastal plain of Samborombón Bay, Argentina. Appl. Geochem. (2013), http://dx.doi.org/10.1016/j.apgeochem.2013.03.006

arbitrary composition of the continental and estuarine water mixing line, would move towards heavier isotopic compositions and lower salinity values. Consequently, additional dissolution of halite is considered when explaining such an extraordinary increase in salinity. Indeed, the $\delta^{18}O$–$\delta^{2}H$ plot indicates that these samples would correspond to low evaporation fractions.

Marsh areas thus have a complex hydrological evolution that may not reach steady values over time, as input from any of the two end members may occur before complete desiccation. Moreover, each water body shows a distinct progression according to its own hydromorphological characteristics. This justifies the large range of chemical and isotopic parameters found in the samples.

The hydrochemical facies and isotopic data in tidal plain groundwater are similar to the ones in the shell ridge (Fig. 10). However, those from the tidal plain show larger variability, which is attributed to the lithological heterogeneity of those sediments. In fact, tidal plain samples have a slightly higher salinity, which is attributed to water–rock interaction, mainly by cation exchange, and also by silicate dissolution. The higher content of Na^+ compared to Cl^- does not support the contribution of estuarine water, and it highlights the occurrence of cation exchange processes where Na^+ is released against Ca^{2+} and Mg^{2+} adsorption. Chloride variability at generally low concentrations (<12 meq/L) cannot be attributed to relic salty pore water or to estuarine influences. Sulfate concentration is also generally low (below 3.0 meq/L), and the Ca^{2-}/SO_4^{2-} ratio varies over a wide range, from 0.56 to 2.25, suggesting a control of Ca^{2-} concentration unrelated to gypsum or calcite equilibrium or even estuarine water influences. Indeed, Na^+ and Ca^{2-} variations lie on a 1:1 line, suggesting that cation exchange explains this shift in their contents in the tidal plain groundwater samples.

Groundwater in the shell ridges results from direct infiltration through the high permeability deposits, with no sign of evaporation as indicated by isotopic values. Due to the hydrogeological parameters, groundwater travel time within the shell ridges is quite short (Carol et al., 2010), as reflected by low salinity values. Carbonate dissolution and cationic exchange are the main processes that determine its hydrochemistry (Fig. 10). During the Holocene, when the sea level dropped, these high permeability sediments formed elevated coastal deposits where Na was progressively released due to the infiltrating rainfall in exchange for Ca derived from organic (shell) carbonate dissolution, as indicated by the following well-known reactions

$$H_2O + CO_{2(g)} + CaCO_3 \leftrightarrow Ca^{2+} + 2HCO_3^-$$

and

$$X\text{-}Na + Ca^{2+} \leftrightarrow X\text{-}Ca + 2Na^+$$

Continuous recharge has deleted additional evidence of its marine origin, resulting in low Cl^-, Mg^{2+} and SO_4^{2-} concentrations consistent with continental freshwater. In addition, incongruent dissolution of albite to kaolinite, montmorillonite and/or gibbsite, identified by mineralogical analysis, may potentially contribute to the groundwater Na^+ and HCO_3^- content (Kortatsi, 2006).

$$\underset{\text{albite}}{2NaAlSi_3O_8} + 2CO_2 + 11H_2O \leftrightarrow \underset{\text{kaolinite}}{Al_2Si_2O_5(OH)_4} + 2Na^+ + 2HCO_3^- + 4H_4SiO_4$$

$$\underset{\text{albite}}{2NaAlSi_3O_8} + Mg^{2+} + 4H_2O \leftrightarrow \underset{\text{montmorillonite}}{2Na_{0.5}Al_{1.5}Mg_{0.5}Si_4O_{10}(OH)_2} + 2Na^+ + 4H_4SiO_4$$

$$\underset{\text{albite}}{NaAlSi_3O_8} + CO_2 + 8H_2O \leftrightarrow \underset{\text{gibbsite}}{Al(OH)_3} + Na^+ + HCO_3^- + 3H_4SiO_4.$$

6. Conclusions

Wetland hydrology in the Samborombón Bay has distinct features for each of the geomorphic units that constitute its structure; namely, the shell ridge, tidal plain and marsh areas close to the bay. Each of them has specific hydrochemical and isotopic characteristics that make it possible to identify the origin of their recharge and the evolution of their water resources.

The shell ridges constitute the main fresh groundwater resources. Due to their relative elevation over this predominantly flat area, a groundwater flow develops towards the nearby tidal flat or marsh areas. Its hydrochemistry is the result of water–rock interaction with no relationship with estuarine water, whereas their isotopic composition is consistent with local rainfall. The tidal plain water samples are hydrochemically and isotopically similar to those of the shell ridges, which do not show any evidence of surface water infiltration from the drainage network.

Groundwater collected in the wells from the marsh areas originates from surface water infiltration, which is enhanced by the burrowing activity of invertebrate wildlife, mainly crabs. Such groundwater indicates the occurrence of different hydrological processes that take place in the marsh water, such as mixing between continental and estuarine water, incipient evaporation and salinity enrichment by halite dissolution precipitated during dry periods.

Surface waters from the Salado River, as well as other streams and canals, show mixing between continental and estuarine water caused by tidal influence. The continental contribution is about 30%, according to the salinity mass balance. Chemical and isotopic evaporation modeling indicates that 15–20% of the surface water evaporates under high humidity conditions (>90%).

This characterization of the coastal hydrology along the Samborombón Bay coast reveals the relevance of the shell ridges as the main groundwater reserves. More importantly, the divergent flow system from these units towards the tidal plain and the marsh areas provides a freshwater flux. Consequently, the environmental quality of surface waters depends on this recharge to maintain biodiversity. Moreover, streams and tidal channels drain the tidal plain, thus controlling the water flow from the plain.

A comprehensive description of the hydrodynamics of this coastal wetland system, based on hydrochemical and isotopic data, exposes the interdependence of all these hydrological units. Consequently, the hydrology of the area should be protected from further human pressure in order to preserve the natural value of these coastal areas.

Acknowledgements

This research was funded by the Consejo Nacional de Investigaciones Científicas y Técnicas (National Council for Scientific and Technological Research) of Argentina. The authors want to express their respect and gratitude to the late Prof. Giovanni Maria Zuppi, who intensively encouraged cooperation among research groups in Europe and Latin America and played a key role in the development of this research.

References

Acha, M., Mianzan, H., Guerrero, R., Carreto, J., Giberto, D., Montoya, N., Carignan, M., 2008. An overview of physical and ecological processes in the Río de la Plata Estuary. Continent. Shelf Res. 28, 1579–1588.

Adamus, P.R., Stockwell, L.T., Clairain Jr. E.J., Morrow, M.E., Rozas, L.P., Smith, R.D., 1991. Wetland Evaluation Technique (WET); vol. 1: Literature Review and Evaluation Rationale. Environmental Laboratory, US Army Engineer Waterways Experiment Station, Vicksburg, MS.

APHA (American Public Health Association),, 1998. Standard Methods for the Examination of Water and Wastewater, 20th ed. American Public Health Association, American Water Works Association, Water Environment Federation, Washington, DC.

Appelo, C.A.J., 1994. Cation and proton exchange, pH variations, and carbonate reactions in a freshening aquifer. Water Resour. Res. 30, 2793–2805.
Barbier, E.B., Acreman, M., Knowler, D., 1997. Economic Evaluation of Wetlands: A Guide for Policy Makers and Planners. Ramsar Convention Bureau, Gland, CH, pp. 1–27.
Barros, V.G., Mas-Pla, J., Novais, T., Sacchi, E., Zuppi, G.M., 2008. Spatial variations of environmental tracers distributions in water from mangrove ecosystem: the case of Babitonga Bay (Santa Caterina, Brazil). Continent. Shelf Res. 28, 682–695.
Carol, E., Kruse, E., Roig, A., 2010. Groundwater travel time in the freshwater lenses of Samborombón Bay, Argentina. J. Hydrol. Sci. 55, 754–762.
Carol, E., Kruse, E., Pousa, J., 2011. Influence of the geologic and geomorphologic characteristics and of crab burrows on the interrelation between surface water and groundwater in an estuarine coastal wetland. J. Hydrol. 403, 234–241.
Coleman, M., Sheperd, T., Durham, J., Rouse, J., Moore, F., 1982. A rapid and precise technique for reduction of water with zinc for hydrogen isotope analysis. Anal. Chem. 54, 993–995.
Craig, H., Gordon, L.I., 1965. Deuterium and oxygen variations in the ocean and the marine atmosphere. In: Tongiorgi, E. (Ed.), Stable Isotopes in Oceanographic Studies and Paleo-Temperatures. CNR Lab. Geol. Nucl., Pisa, pp. 9–130.
Custodio, E., 2010. Coastal aquifers of Europe: an overview. Hydrogeol. J. 18, 269–280.
Dapeña, C., Panarello, H., 2004. Composición isotópica de la lluvia de Buenos Aires. Su importancia para el estudio de los sistemas hidrológicos pampeanos. Rev. Lat. Am. Hidrogeol. 4, 17–25.
Edmunds, W.M., 1996. Bromide geochemistry of British groundwaters. Mineral. Mag. 60, 275–284.
Gonfiantini, R., 1978. Standard for stable isotope measurements in natural compounds. Nature 271, 534–536.
Gonfiantini, R., 1986. Environmental isotopes in lake studies. In: Fritz, P., Fontes, J.C. (Eds.), Handbook of Environmental Isotope Geochemistry, vol. 2. Elsevier Scientific, pp. 113–167.
Kakiuchi, M., Matsuo, S., 1979. Direct measurements of D/H and $^{18}O/^{16}O$ fractionation factors between vapor and liquid water in the temperature range of 10 to 40 °C. Geochem. J. 13, 307–311.
Kortatsi, B., 2006. Hydrochemical characterization of groundwater in the Accra plains of Ghana. Environ. Geol. 50, 299–311.
Kruse, E., Mas-Pla, J., 2009. Procesos hidrogeológicos y calidad del agua en acuíferos litorales. In: Mas-Pla, J., Zuppi, G.M. (Eds.), Gestión ambiental integrada de áreas costeras. Rubes Editorial, Barcelona, pp. 29–53.
LePage, B.A., 2011. Wetlands. Integrating Multidisciplinary Concept. Springer.
Panarello, H., Paricia, C., 1984. Isótopos del oxígeno en hidrogeología e hidrología. Primeros valores en agua de lluvia de Buenos Aires. Rev. Asoc. Geol. Argentina 34, 3–11.
Parker, G., 1979. Geología de la planicie costera entre Pinamar y Mar de Ajó, provincia de Buenos Aires. Rev. Asoc. Geol. Argentina 34, 167–183.
Parkhurst, D.L., Appelo, C.A.J., 1999. User's Guide to PHREEQC (Version 2). A Computer Program for Speciation, Batch-reaction, One-dimensional Transport, and Inverse Geochemical Calculations: US Geol. Surv. Water-Resour. Invest. Rep. 99-4259.
Pera-Ibarguren, S., 2004. Surface Water – Groundwater Interactions in Transition Environments: The Río de la Plata Coastal Plain, Argentina. PhD Dissertation. Univ. Ca' Foscari Venezia, Italy.
Pousa, J., Kruse, E., Carol, E., Carretero, S., Guaraglia, D., 2011. Interrelation between coastal processes surface water and groundwater at the outer coastal region of the Río de la Plata Estuary, Argentina. In: Daniels, J.A. (Ed.), Advances in Environmental Research, vol. 10. Nova Science Publishers, Hauppauge, New York, USA, pp. 67–96.
Violante, R., Parker, G., Cavallotto, J., 2001. Evolución de las llanuras costeras del este bonaerense entre la bahía de Samborombón y la laguna de Mar Chiquita durante el Holoceno. Rev. Asoc. Geol. Argentina 56, 51–66.

Please cite this article in press as: Carol, E., et al. Interaction between continental and estuarine waters in the wetlands of the northern coastal plain of Samborombón Bay, Argentina. Appl. Geochem. (2013), http://dx.doi.org/10.1016/j.apgeochem.2013.03.006